Digital-to-Optical Converters (DOCs) with Improved Nonlinearity for Energy-Efficient Optical Data Transmission

John Davis[1], Georgios Kyriazidis[1], Yaowen Hu[1,2], Hana Warner[1], Xinrui Zhu[1], Leticia Magalhaes[1], Melinda Modisette[1], Norman Lippok[1,3], Kiyoul Yang[1], Benjamin Vakoc[3], Marko Lončar[1], Gage Hills[1]

[1]Harvard School of Engineering and Applied Sciences (SEAS), Cambridge, Massachusetts, USA
[2]Peking University, Beijing, China
[3]Wellman Center for Photomedicine, Boston, Massachusetts, USA

Abstract

Digital-to-Optical Converters (DOCs) convert *digital electrical signals* directly to *analog optical signals*, eliminating the need for Digital-to-Analog Converters (DACs) in Electro-Optic (EO) modulators, for applications in energy-efficient data communication. However, nonlinearity in DOCs degrades Symbol Error Rate (SER), power, and bandwidth. We present *Engineered-Segment Length (ESL) DOC* circuits that achieve strictly better trade-offs in Integral Non-Linearity (INL), Differential Non-Linearity (DNL), SER, and optical power vs. state-of-the-art DOC circuits. We experimentally demonstrate DOCs in heterogeneously integrated Si CMOS and Thin-Film Lithium Niobate (TFLN). Our measured ESL DOCs improve Root-Mean-Square (RMS) INL from 1.04 to 0.14 Least-Significant Bits (LSBs) and RMS Differential Non-Linearity (DNL) from 0.42 to 0.10 LSBs.

Introduction

Electronic-Photonic Integrated Circuits (EPICs) have enabled high communication baud rates (symbol rates) of 100 Gbaud/s and beyond [1], by leveraging on-chip EO modulators (e.g., Mach-Zehnder Modulators or MZMs) in material platforms such as Silicon Photonics [2] and TFLN for high-bandwidth photonics [3]. Baud rates for EO transmitter (Tx) circuits are now limited by electrical drive circuits, leading designers to encode multiple bits per symbol to increase the overall bit rate, e.g., 4-level Pulse Amplitude Modulation (PAM4) [4], and more general intensity/quadrature constellations [5]. A key drawback for these multi-bit protocols, however, is that Tx circuits often require DACs, which have become major bottlenecks in terms of: (a) optical power or energy per bit, (b) latency or bandwidth, and (c) design complexity.

Toward addressing this challenge, DOCs have enabled Tx circuits to encode multiple bits per symbol *without requiring DACs*. In contrast to analog voltage-driven EO modulators, whose optical power corresponds to the analog voltage inputs on a set of electrodes (Fig. 1), DOCs leverage EO modulators where each electrode is split into multiple segments, each of which is driven with by an independent voltage input [6]. The optical power output corresponds to the total modulated electrode length over all segments (Fig. 2). This segmentation allows EO modulators to be driven digitally without the need for electronic DACs. However, due to the nonlinear transfer function of transmitted optical power vs. MZM input voltage (details below), DOCs have suffered from high INL and DNL. For EO Tx circuits, this corresponds to a smaller separation between transmitted optical power levels, which exacerbates Inter-Symbol Interference (ISI), ultimately degrading trade-offs in SER, optical power, and communication bandwidth. Our *ESL DOCs* overcome these challenges through careful engineering of the segmented electrode lengths to achieve evenly spaced optical power levels, minimizing INL and DNL.

Operation of DOC Circuits

Figure 1 summarizes three strategies for driving MZMs. MZM driver electrodes induce a phase shift proportional to the product of the operating voltage and modulator length. Typical analog MZMs modulate light by varying only the input voltage. Electrode segmentation varies the modulator's effective length instead, enabling input voltages to be driven to one of two binary values (e.g., VDD or VSS). This permits the use of *digital drivers*, eliminating the need for DACs.

Uniform-length segmentation and binary-weighted-length segmentation schemes [7] vary phase linearly, producing a sinusoidal relationship in output power vs. input code (Fig. 1). This corresponds to non-uniform spacing in output power levels, degrading SER. ESL-DOC solves this problem by linearizing output power vs. digital input code (Fig. 2).

Experimental Results

We compare experimental measurements (Fig. 3) from a 4-bit ESL DOC vs. a 4-bit Binary-Weighted DOC, both implemented in TFLN. Continuous Wave (CW) laser light is modulated by the DOCs (Fig. 4). Measured symbols in Fig. 5 are used to compute INL and DNL for both the ESL and Binary DOC. The ESL DOC shows improved RMS INL of 0.14 LSBs and DNL of 0.10 LSBs.

We quantify SER for both the ESL and Binary-Weighted DOCs by simulating a Gaussian noise profile in optical power around both simulated and measured optical intensities for each code for both DOCs (Fig. 6). Our results (Fig. 7) show that the ESL DOC significantly improves SER compared to the Binary-Weighted DOC for a given Signal-to-Noise Ratio (SNR). ESL DOC requires approximately 5 dB less optical power vs. the Binary-Weighted DOC (non-ESL DOC) for the same SER. Similarly, for the same optical power level, ESL DOC improves SER by approximately 10 orders of magnitude.

As an alternative approach, linearity can be improved in the Binary-Weighted DOC by using an optimal subset of codes from a Binary-Weighted DOC with more bits. This approach, Binary ESL (BESL), offers trade-offs in SER vs SNR that are between those of the Binary-Weighted and ESL DOCs. BESL codes are chosen to minimize ISI by maximizing the minimum distance between adjacent symbol codes in the constellation as demonstrated in Fig. 8.

A practical benefit of segmented MZMs is that they can be driven at high speeds by standard CMOS digital inverter-based drivers, *without* the need for detailed analog circuits. As an illustration, we show circuits simulations that leverage unmodified standard cell libraries from the ASAP7 PDK [8] to drive electrodes in ESL and BESL DOCs. Fig. 9 shows that the ASAP7 libraries enable 25 GHz modulation of 4-bit ESL DOCs using only digital inverters (VDD = 0.7 V). Alternative digital drivers can also be used. We note that conventional optical receiver (Rx) circuits can be used with ESL DOC Tx circuits (i.e., ESL DOCs do not require custom Rx circuits).

Figure 10 shows our fabricated TFLN chip and Si CMOS driver chip. Table 1 summarizes different characteristics of multiple 4-bit DOC configurations.

Conclusion

Our ESL technique improves linearity of transmitted optical power vs. digital input code for DOCs. We show experimentally that ESL enables strictly better trade-offs for SER vs. optical SNR per bit for EO transmitters that use DOCs. Results are measured from our fabricated TFLN chip with both ESL and non-ESL DOCs. ESL can also be applied to alternative EO modulators and material platforms. We show that Binary-Weighted DOCs can be engineered to achieve comparable performance to ESL by removing codes from larger bit-width modulators. We use a 7 nm node PDK to show that simple inverter-based CMOS drivers can drive DOCs at high speeds, with ESL DOCs achieving superior trade-offs in INL, DNL, SER, and optical power due to their inherent linearity of transmitted optical power vs. input digital code.

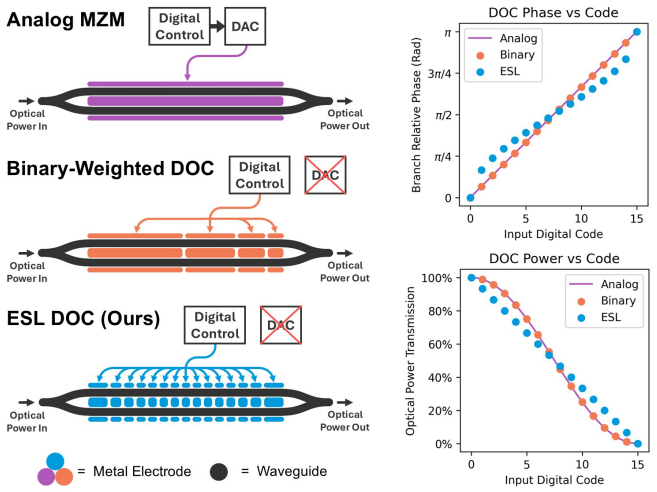

Fig. 1. Different strategies for MZM modulation: Analog, Binary-Weighted, and ESL. The Binary-Weighted and ESL DOCs are driven digitally without the need for a DAC.

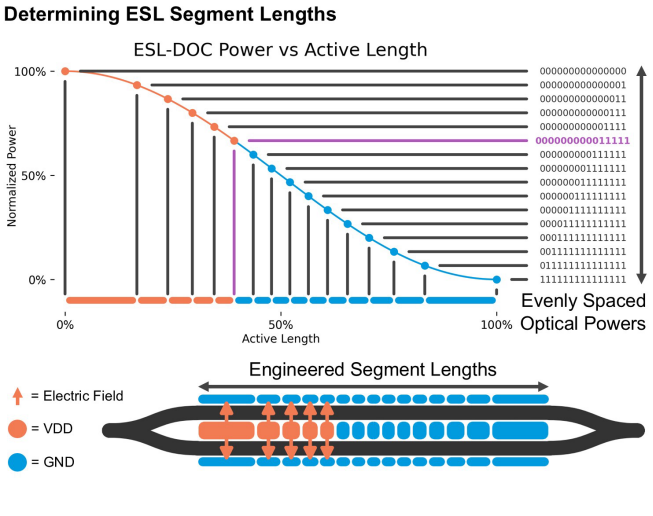

Fig. 2. Design of ESL segment lengths to correct for the sinusoidal power transfer function with respect to MZM active modulation length. Engineered segments yield evenly spaced output powers.

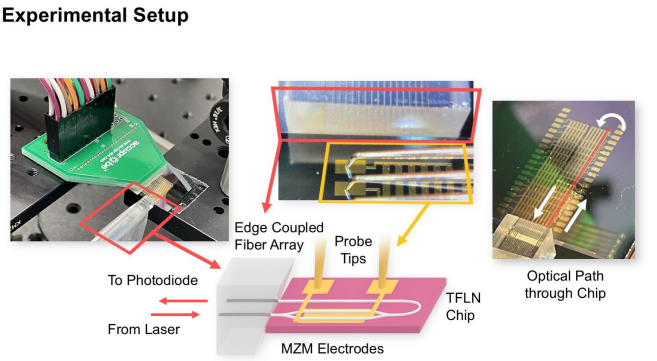

Fig. 3. DOC measurement setup. The TFLN chip edge is polished and connected optically via an edge coupled fiber array. The chip receives digital modulation signals from a probe card which is connected to a custom electronic driver circuit. Input light from the first fiber array channel gets modulated by the chip and is coupled to a second fiber array channel which serves as the output.

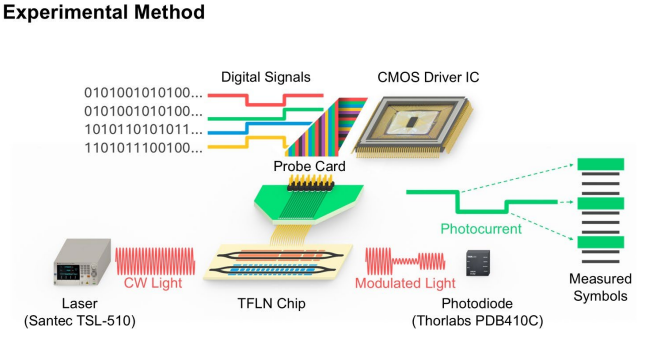

Fig. 4. DOC measurement overview. Continuous wave laser light is modulated by the TFLN chip. The modulated optical amplitude is converted to an electronic signal using a transimpedance amplified photodiode whose output voltage is proportional to measured optical power. The discrete voltage levels at the amplifier output correspond to the measured symbols which are used for nonlinearity and noise analysis in a simulated channel.

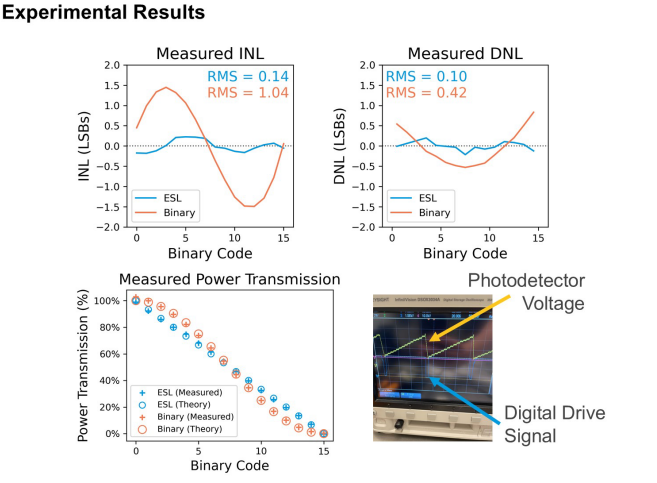

Fig. 5. Measured results from the fabricated TFLN chip showing improved INL and DNL in the ESL DOC. Measured optical power transmission through the ESL DOC follows a linear power profile while the Binary-Weighted DOC is sinusoidal.

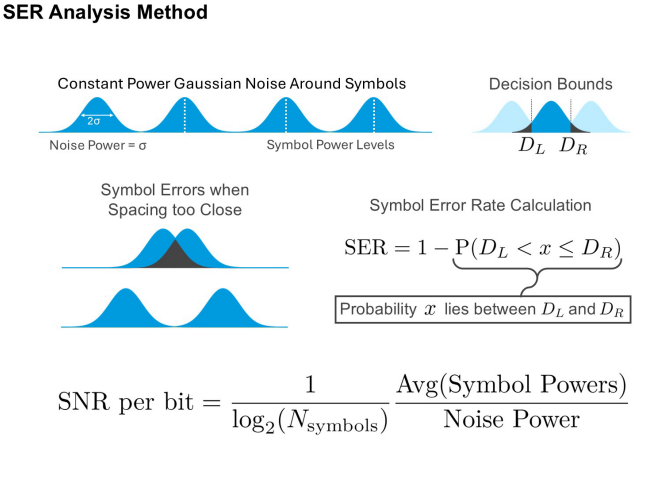

$$\text{SNR per bit} = \frac{1}{\log_2(N_{\text{symbols}})} \frac{\text{Avg(Symbol Powers)}}{\text{Noise Power}}$$

Fig. 6. Method for determining SER from symbol levels using a simulated additive gaussian noise channel. Decision bounds for demodulation are halfway between adjacent symbol power levels. SNR per bit is the optical signal SNR normalized for bits-per-symbol.

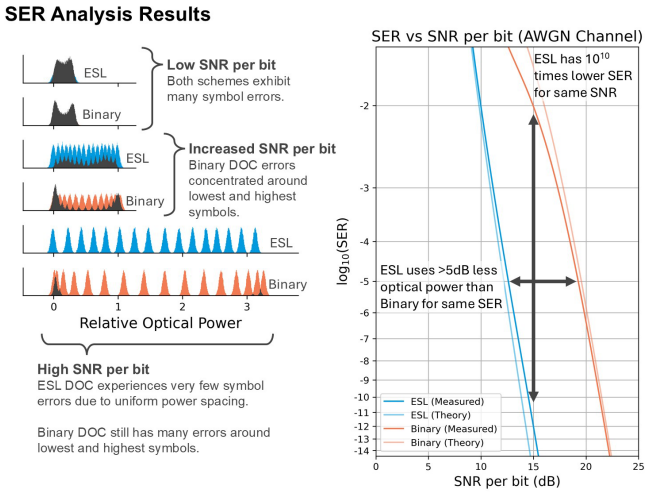

Fig. 7. Results of the SER analysis showing that the ESL DOC achieves a lower SER vs SNR per bit compared to the Binary DOC.

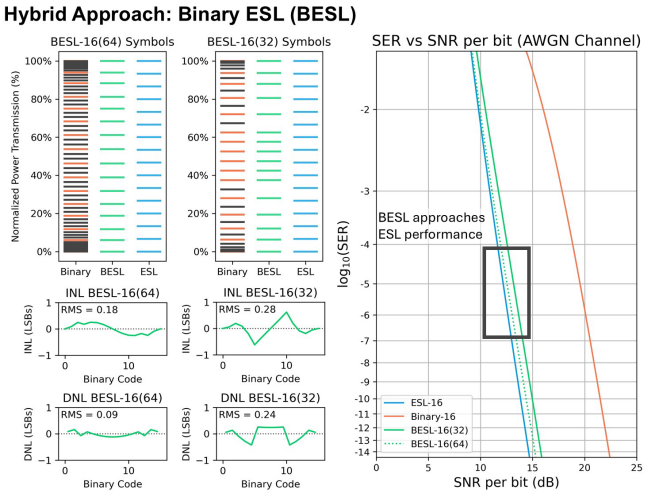

Fig. 8. SER analysis results for BESL where codes are removed from a Binary DOC to approximate an equivalent ESL DOC.

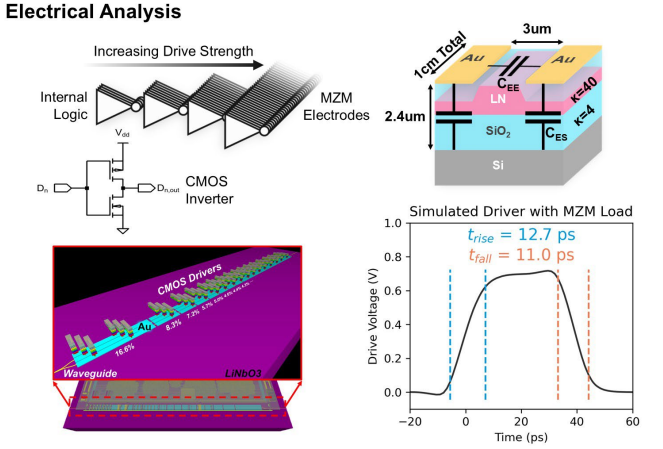

Fig. 9. Electrical driver analysis using the ASAP7 PDK [8] shows that ESL DOC electrodes can achieve 25 GHz modulation. When combined in an 8-color wavelength division multiplexing (WDM) setup, this enables data transmission rates of 800 Gbps (PAM16 with SER of 20.8E-16 for 15dB SNR per bit), showcasing scalability and performance for high-speed optical communication.

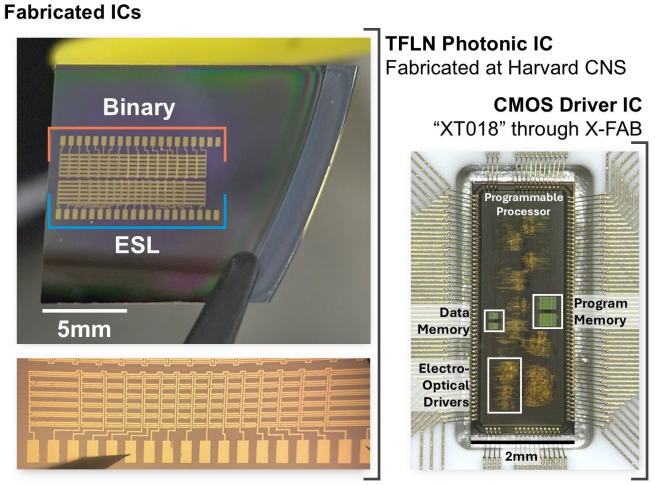

Fig. 10. Fabricated test devices. The TFLN chip has 6 Binary-Weighted and 6 ESL DOCs. The Binary-Weighted DOC is split into segments of equal length to reduce load capacitance for the driver electronics and can be driven by multiple digital pins as necessary.

TABLE I. Comparison table between 4- bit DOC configurations.

	ESL-16	Binary-16	Binary-16 [7]	BESL-16(32)	BESL-16(64)
DOC Bits	4	4	4	5	6
BAUD Rate *ASAP7 PDK*	25GHz	25GHz	**46.5GHz***	25GHz	25GHz
INL (LSB RMS)	**0.14***	**1.04***	1.10	0.28	0.18
DNL (LSB RMS)	**0.10***	**0.42***	0.48	0.24	0.09
Simulated SER *SNR per bit = 15dB*	2.08E-16	2.22E-2	2.22E-2	2.08E-10	5.82E-13

*** Measured Data**

References

[1] S. Shekhar et al., "Roadmapping the next generation of silicon photonics," Nature Comm., vol. 15, no. 1, p. 751, 2024.

[2] R. Soref and J. Lorenzo, "Single-crystal silicon: a new material for 1.3 and 1.6 µm integrated-optical components," Electronics Letters, vol. 21, no. 21, pp. 953–954, 1985.

[3] D. Zhu et al., "Integrated photonics on thin-film lithium niobate," Advances in Optics and Photonics, vol. 13, no. 2, pp. 242–352, 2021.

[4] J. Wang et al., "7.1 a 2.69 pj/b 212gb/s dsp-based pam-4 transceiver for optical direct-detect application in 5nm finfet," IEEE ISSCC, vol. 67, pp. 123–125, 2024.

[5] Y. Ding, H. Wang, and Y. Ji, "High-speed all-optical constellation add-drop multiplexer for 16-qam based on constellation update in elastic optical networks," Optics & Laser Technology, vol. 169, p. 110028, 2024.

[6] T. N. Huynh et al., "Flexible transmitter employing silicon-segmented mach–zehnder modulator with 32-nm cmos distributed driver," Journal of Lightwave Technology, vol. 34, no. 22, pp. 5129–5136, 2016.

[7] Y. Song et al., "Integrated electro-optic digital-to-analog link for efficient computing and arbitrary waveform generation," arXiv, 2024.

[8] L. T. Clark et al., "Asap7: A 7-nm finfet predictive process design kit," Microelectronics Journal, vol. 53, pp. 105–115, 2016.